Evidence for parity violation in gravitational fields

V. Gharibyan,[1] V. Adler,[1] P.D. Allfrey,[2] M.A. Bell,[2] B.D. Belusic,[1] A. Block,[1] Y. Bozhko,[1] J.A. Coughlan,[3] R.K. Dementiev,[4] A. Deshpande,[5] J. Ferencei,[6] R. Gonçalo,[7] K.H. Hiller,[8] R. Kaiser,[9] R. Kammering,[1] B. Krause,[1] B.-Q. Ma,[10] M.C.K. Mattingly,[11] S. Padhi,[12] A. Perieanu,[13] D. Protopopescu,[14] P. Ryan,[15] J. Schaffran,[1] P. Schmid,[1] M. Seebach,[1] E. Sombrowski,[1] G. Susinno,[16] M. Wang,[17] K. Wick,[13] M. Wobisch,[18] and A. Zichichi[19]

[1] *Deutsches Elektronen-Synchrotron DESY, Hamburg, Germany*
[2] *Department of Physics, University of Oxford, Oxford, United Kingdom*
[3] *Rutherford Appleton Laboratory, Chilton, Didcot, United Kingdom*
[4] *Moscow State University, Institute of Nuclear Physics, Moscow, Russia*
[5] *Department of Physics, Yale University, New Haven, Connecticut 06520-8121, USA*
[6] *Institute of Experimental Physics, Slovak Academy of Sciences, Košice, Slovak Republic*
[7] *Laboratrio de Fsica Experimental de Partculas, Av. Prof. Gama Pinto 2, 1649-003 Lisboa, Portugal*
[8] *Deutsches Elektronen-Synchrotron DESY, Zeuthen, Germany*
[9] *Department of Physics and Astronomy, University of Glasgow, Glasgow, United Kingdom*
[10] *School of Physics, Peking University, Beijing 100871, China*
[11] *Andrews University, Berrien Springs, Michigan 49104-0380, USA*
[12] *Department of Physics, McGill University, Montréal, Québec, Canada H3A 2T8*
[13] *Institut für Experimentalphysik, Universität Hamburg, Hamburg, Germany*
[14] *School of Physics and Astronomy, University of Glasgow, Glasgow G12 8QQ, United Kingdom*
[15] *Department of Physics, University of Wisconsin, Madison, Wisconsin 53706, USA*
[16] *Calabria University, Physics Department and INFN, Cosenza, Italy*
[17] *Physikalisches Institut der Universität Bonn, Bonn, Germany*
[18] *Louisiana Tech University, Ruston, Louisiana 71272, USA*
[19] *University and INFN Bologna, Bologna, Italy*

Discrete symmetries in gravity have only been tested for low energy, non-relativistic matter, confirming the perfectly symmetric general relativity. A hint for high energy $\mathcal{CP}$ violation in gravitational fields has recently been found in the HERA Compton polarimeter's two spectra, measured with electron and positron beams. Here we report results of the analysis of the same polarimeter's 314896 spectra, acquired during 2004–2007 and tagged by laser polarization states allowing the separation of charge ($\mathcal{C}$) and space ($\mathcal{P}$) parity contributions. The measured Compton edge energy asymmetry, induced by the laser helicity flips, is as high as $(4.9 \pm 0.5) \cdot 10^{-5}$ which corresponds to a helicity-dependent difference in the gravitational potentials of $(1.7 \pm 0.2) \cdot 10^{-14}$. In the case of the observed anomalous coupling's energy independence, the spin asymmetric gravity will contribute to the galactic rotational curves and the cosmic microwave background. Further analysis and calculations can determine whether the observed magnitude of the gravitational parity violation is sufficient for detaching these famous phenomena from the dark matter and the Big Bang theory.

PACS numbers: 04.80.Cc, 11.30.Er, 41.75.Ht

INTRODUCTION

General Relativity (GR) [1], the currently accepted theory of gravitation, rests on the principle of equivalence, which is a concept originating from the universality of free fall for massive bodies. Up to now all macroscopic scale experiments have confirmed this basic gravitational principle down to the contemporary limit of 10^{-13} [2, 3]. In the microscopic realm of quantum and high-energy physics the gravitation is completely negligible in comparison to the nuclear or electroweak forces between the particles. Also the influence of gravity as an external field is largely ignorable for quantum particle interactions. Indeed, according to the equivalence principle, particles with different natures, intrinsic, spatial, or energetic properties are affected (accelerated) equally by gravity. Such absolute democracy and symmetry makes any gravitational field undetectable for high energy particle interactions taking place at a local space-time point. The situation is different if the symmetry is broken. Then an instantaneous momentum exchange with the background gravitational field will depend on the particle's type and features affecting the quantum processes' kinematics and dynamics. We are searching for such asymmetries in gravity, motivated by particle physics' well known observations that the weaker interactions are less symmetric.

Recent calculations [4] demonstrate a considerable sensitivity of the high energy Compton scattering to the gravitational field's broken symmetries. Using two Compton spectra measured by the HERA transverse polarimeter, a signature for gravitational $\mathcal{CP}$ violation has been extracted in the same ref. [4]. These spectra have been obtained from unpolarized laser–electron and left helicity laser–positron scatterings. The reported upper limit of the gravitational parity ($\mathcal{P}$) violation is

$(1.3 \pm 0.3) \cdot 10^{-11}$ at 13 GeV energies. At low energies, most of the existing $\mathcal{P}$-asymmetric gravity limitations are model dependent and set by precise spectroscopic or polarized torsion pendulum [5] experiments. They constrain hypotheses such as Lorentz violation [6], torsion gravity [7], exchange of pseudoscalar bosons [8], and a few others. A detailed review [9] for low energy spin-dependent gravitation quotes a current best limit around 10^{-7}.

In this paper we will follow the formalism developed in ref. [4] to evaluate high energy laser-Compton scattering's analyzing power for gravity's left–right preference in a model-independent manner. After a short description of the HERA transverse polarimeter setup we will explore the polarized Compton spectra sampled during the 2004–2007 running period to extract the Compton edge left–right energy asymmetry and derive the magnitude of the gravitational space parity violation. At the end we will discuss the detected $\mathcal{P}$-asymmetric gravitation's possible impact on some interpretations of astrophysical data.

GRAVITATIONAL REFRACTIVITY

An external gravitational field with a Newtonian potential U modifies the momentum P and energy $\mathcal{E}$ relation of a particle via the expression

$$c\frac{P}{\mathcal{E}} = \frac{v}{c} - \frac{2U}{c^2} + \mathcal{O}\Big(\frac{U^2}{c^4}\Big), \tag{1}$$

where v is the speed of the particle and c is the speed of light. This gravitational refraction[1] is derived from GR for weak fields, when the Schwarzschild metric is replaced by the field's potential $U = -GM/R$ for the particle at a distance R from the gravitating mass M [4, 10]. Within GR all phenomena are described by Einstein's equation, expressing energy-momentum conservation in curved space-time. In weak fields, Eq. (1) together with energy-momentum conservation is sufficient for evaluating all gravitational effects. In a laboratory, the major attractors create fields with $U/c^2 \ll 1$ (see table I) and the resulting field ΣU could also be described in terms of a flat space refractivity. In Eq. (1), the equivalence principle manifests itself by the independence of the gravitational constant G, and the potential in general, on whatever property of the particle. This leads to cancellation of the gravitational potential in energy-momentum conservation for any initial and final states at the quantum particles' interaction vertex. Since any observable has to be gauge invariant, the gravitational measurables can only depend on potential differences

$$\Delta U(G, M, R) = U\frac{\Delta G}{G} + U\frac{\Delta M}{M} - U\frac{\Delta R}{R}, \tag{2}$$

where the first term $\Delta U_G \equiv U\Delta G/G$ violates gravitational equivalence between different particles or states. In GR $\Delta U_G = 0$ and experimentally it is constrained exceptionally by low energy tests. The second term with mass change is currently not associated with any known test or system and the third term $\Delta U_R \equiv U\Delta R/R$ is responsible for the conventional gravitational effects: the particles' deflection and frequency shift. Typical magnitudes of these effects for relativistic particles at the Earth's surface are proportional to the potential difference ΔU_R presented in table I. So far only the vertically moving (keV) photons' frequency change has been measured using the nuclear Mössbauer detectors [11]. High energy particles' (or light's) deflection $2L\Delta U_R/c^2$ over a horizontal distance L is out of reach of any laboratory instrumentation even for $L \sim$ km scale.

TABLE I. Gravitational fields and gradients (per one meter) at laboratory. Listed are only the dominant contributors: the Earth, the Sun, the Milky Way, and the Local (Virgo) Supercluster.

Potential \ Source	Earth	Sun	Galaxy	Virgo SC
U/c^2	$7 \cdot 10^{-10}$	$9 \cdot 10^{-9}$	$3 \cdot 10^{-7}$	$3 \cdot 10^{-5}$
$\Delta U_R/c^2/m$	10^{-16}	$7 \cdot 10^{-29}$	10^{-27}	10^{-36}

In order to quantify and measure the space parity violation induced by gravitation, let's assume a spin-dependent gravity with different couplings to the left and right helicity particles. For this purpose, we introduce an interaction constant

$$G_s = G + \frac{\mathbf{s}\cdot\mathbf{P}}{P}\Delta G_{\mathcal{P}}, \tag{3}$$

which couples the gravitational field to the particles with spin $\mathbf{s}$. This basic and minimal assumption will modify Eq. (1) to

$$c\frac{P}{\mathcal{E}} = \frac{v}{c} - \frac{2}{c^2}\Big(U + \Delta U_{\mathcal{P}}\Big), \tag{4}$$

with a space parity violating term

$$\Delta U_{\mathcal{P}} = \frac{\mathbf{s}\cdot\mathbf{P}}{P}U\frac{\Delta G_{\mathcal{P}}}{G} \tag{5}$$

The helicity $(\mathbf{s}\cdot\mathbf{P}/P)$ dependent interaction is assumed to be small, so that $\Delta G_{\mathcal{P}}/G \ll 1$. We also note that the introduced deviation from the equivalence principle is Lorentz invariant ($v \leq c$) and does not violate Special Relativity (SR). The specified mirror-symmetry breaking

[1] The terminology originates from optics (for $v = c$). Since the right side of Eq. (1) is energy independent, gravity is not dispersive.

gravity will potentially affect all polarized interactions in a gravitational field through the relation (4), while the second term in this relation is not universal anymore and depends on the interacting particle's spin state. From Eq. (4) it also follows that the term with $\Delta U_{\mathcal{P}}$ primarily affects the velocity of the particle. Hence, mainly the high energy processes would have sufficient sensitivity to detect the gravitational $\mathcal{P}$-parity violation through introduced velocity change given the well-known SR relation

$$\frac{\mathcal{E}^2}{m^2}\cdot\frac{dv}{v}=\frac{c^2}{v^2}\cdot\frac{d\mathcal{E}}{\mathcal{E}}, \tag{6}$$

with the particle mass m. This relation amplifies any tiny relative change in velocity $\Delta v/v$ by the Lorentz factor $\gamma=\mathcal{E}/m$ quadrature connecting it to a potentially detectable energy change $\Delta\mathcal{E}/\mathcal{E}=(\gamma^2-1)\Delta v/v$.

HIGH ENERGY COMPTON SCATTERING IN A GRAVITATIONAL FIELD

Consider the polarized Compton process when a laser photon with energy ω_0 and helicity λ scatters off an accelerated lepton with high energy $\mathcal{E}$ and zero helicity (from here on natural units are used). Then, the scattered photon with maximum energy ω_{max} (at the Compton edge) will retain the initial helicity [12] while the secondary lepton will acquire a helicity $\lambda_l=-\lambda x(2+x)/(1+(1+x)^2)$, according to refs. [13, 14]. The Compton kinematic factor $x=4\gamma\omega_0\sin^2(\theta_0/2)/m$, is defined for an initial photon–lepton interaction angle θ_0. Assuming the scattering takes place in a gravitational field which violates $\mathcal{P}$-parity by an amount of $\Delta U_{\mathcal{P}}$, we apply Eq. (4) to all initial and final particles. After lengthy but simple calculations, the energy-momentum conservation reads

$$x-y(1+x)-2(y^2(\lambda_l-2)-2y(\lambda_l-1)+\lambda_l)\gamma^2\lambda\Delta U_{\mathcal{P}}=0, \tag{7}$$

where $y=\omega_{max}/\mathcal{E}$ is the maximum relative energy of the scattered photon and the $\mathcal{O}(\gamma^{-3})$ terms are neglected. According to this relation, the maximum energy of the scattered gamma particle will depend on the laser helicity and the mirror symmetry breaking gravitation will induce a Compton edge asymmetry

$$A=\frac{\omega^-_{max}-\omega^+_{max}}{\omega^-_{max}+\omega^+_{max}}, \tag{8}$$

where the upper indices denote the helicity states. From Eq. (7) there follows

$$A=\frac{2u(x^2+2x+2)}{-x^4-4x^3-7x^2+(u-6)x+2u-2}, \tag{9}$$

with the assignment $u\equiv-2\gamma^2\Delta U_{\mathcal{P}}$. And, inversely, from a measured Compton edge spin asymmetry A one can derive the gravitational left–right helicity potential's difference

$$\Delta U_{\mathcal{P}}=\frac{1}{2\gamma^2}\cdot\frac{A(x^2+2x+2)(x+1)^2}{2x^2+(4-A)x-2A+4}. \tag{10}$$

In the above relations the amplification factor γ^2 sets the detection scale for the high energy Compton process to measure the gravitational parity violation. In order to estimate the sensitivity of the laser-Compton scattering we insert the parameters of the HERA transverse polarimeter setup (see the next section) into Eq. (9). For a range of feasible left–right helicity asymmetry measurements one can refer to high energy precise detectors. Measurements of asymmetries as low as 10^{-7} have been reported at SLAC 50 GeV [15, 16] or at MAMI 1 GeV experiments [17, 18]. Hence, for the sensitivity plot presented by Fig. 1, we conservatively use a lower asymmetry value of $5\cdot10^{-6}$.

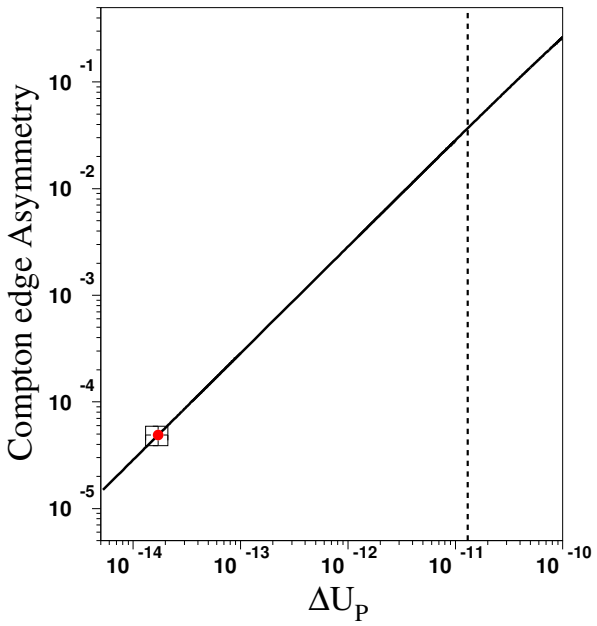

FIG. 1. The sensitivity of the Compton photons' maximum energy to the gravitational field helicity dependent coupling (potential difference $\Delta U_{\mathcal{P}}=U_{Left}-U_{Right}$) for the HERA transverse polarimeter. The dashed vertical line indicates an upper limit detected in ref. [4]. The experimental result of this paper is shown by the point with error box.

EXPERIMENTAL SETUP

The HERA transverse polarimeter is built to measure the average vertical spin of the circulating electrons or positrons using spatial and energy spectra from polarized laser Compton scattering. The spectra have been

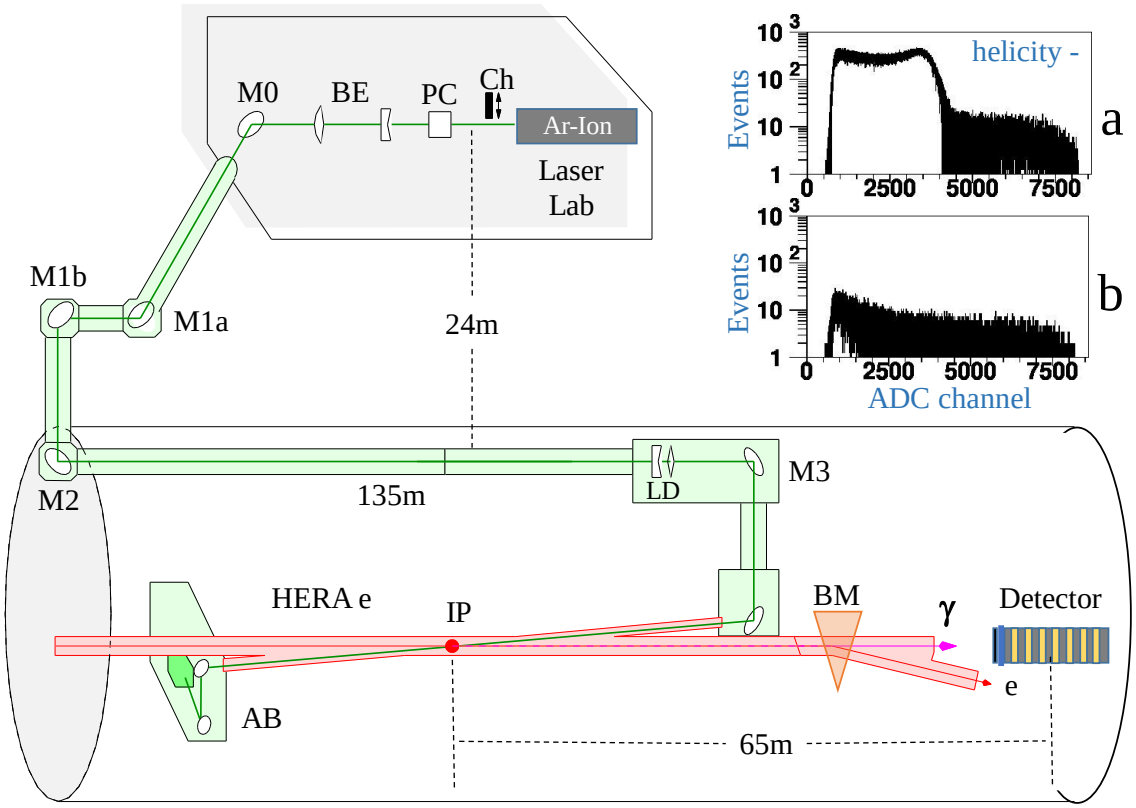

FIG. 2. Simplified outline of the HERA transverse polarimeter. The setup elements displayed in the Laser Lab and HERA tunnel are: light Chopper-shutter (Ch), Pockels Cell (PC), Beam Expander (BE), Mirrors (M0–M3), Lens Doublet (LD), light Analyzer Box (AB), laser–lepton Interaction Point (IP) and Bending dipole Magnet (BM). *Inset (a)*: Raw Compton spectrum measured with left helicity laser during 45 sec shutter open cycle. *Inset (b)*: Background Bremsstrahlung spectrum sampled during 15 sec shutter closed period.

sampled by directing 514.5 nm laser light against the HERA 27.6 GeV electron beam with a vertical crossing angle of 3.1 mrad and detecting the produced high energy γ-quanta with a segmented calorimeter. The listed initial conditions correspond to the kinematic parameter $x = 1.02$ and Compton edge $\omega_{max} = 13.9$ GeV for the scattered photon beam. A reduced layout of the polarimeter setup is shown in Fig. 2. The whole detection scheme is designed for the measurement of an up–down spatial asymmetry of the γ-quanta which is introduced by a flip of the laser light's helicity and is proportional to the lepton beam transverse polarization. The laser (Coherent Sabre Argon Ion) produces 10 W CW linearly polarized light in TEM_{00} mode. The linear (linearly polarized) light is converted to circular (circularly polarized) by a Pockels cell with 85 Hz switching between positive and negative helicities. A mechanical chopper periodically blocks the laser beam shutting the light off for 15 sec within each 1 min measurement cycle in order to sample the background spectra. An evacuated transport system with remotely controlled mirrors delivers the laser light about 200 m from the optical lab to the Compton interaction point (IP). The laser beam is expanded (1:10) before the transport for focusing into the lepton beam by a lens-doublet installed 18.4 m upstream the IP. An analyzer optical setup at the laser beam-dump monitors the remnant of linear light to optimize the circular polarization magnitude at the laser–lepton interaction point.

The energy measurement of the Compton γ-quanta is auxiliary and serves as a means to enhance the spatial asymmetry by imposed energy cuts. Since we are going to compare the maximum energies of the photons from the Compton spectra tagged by light helicity we concentrate on those details of the experimental setup that are important for energy measurement only, ignoring all features related to the lepton polarization detection.

The scattered Compton photons originate from an interaction region (IR) about 0.5 m long, defined by the crossing angle and size of the electron and laser beams. Bending dipole magnets downstream of the IR separate the electron and γ beams and the photons leave the vacuum pipe through a 0.5 mm thick aluminum window to travel via a mostly evacuated 39 m path before entering the calorimeter, which is installed 65 m downstream the IR. Collimators placed at a distance of 47 m from the IR define an aperture of ± 0.37 mrad, the same as

the angular size of the calorimeter as seen from the IR. The aperture is 15 times larger than the largest (horizontal) angular spread of electrons at the IR and 40 times larger than the characteristic radiation angle $1/\gamma$, so the acceptance inefficiency can be ignored. The collimators are followed by magnets to sweep out any charged background.

The calorimeter consists of 12 layers of 6.2-mm thick tungsten and 2.6-mm thick scintillator plates surrounded by four wavelength shifters attached to four photomultipliers (PMT). A converter-preshower tungsten plate with one radiation length, installed in front of the calorimeter, provides charged particles for the operation of position-sensitive silicon strip detectors.

PMT signals from single photons are stretched by shapers to 96 ns and fed into analog-to-digital converter (ADC) in a 10 MHz data acquisition (DAQ) system similar to the HERA cavity polarimeter DAQ described in ref. [19]. An essential difference from the cavity polarimeter DAQ is the trigger mode operation, which stops the ADC pipeline only for the signals exceeding a given threshold (about 3 GeV).

The detector performance has been simulated with the GEANT Monte Carlo program and tested using DESY and CERN test beams. The measured energy resolution of 24% $\mathrm{GeV}^{1/2}$, spatial non-uniformity of $\pm 1\%$, and nonlinearity of 2% at 20 GeV are in agreement with the simulations.

Apart from the laser light, the lepton beam also interacts with residual gas, thermal photons, and the bending magnetic field in the beam pipe, producing, respectively, Bremsstrahlung, scattered blackbody radiation, and synchrotron radiation reaching the calorimeter. To measure this background, the laser beam is blocked for 15 sec of each 1 min measurement cycle (laser light on/off is 45/15 sec). This procedure allows eliminating the background by a simple subtraction of time normalized light-off spectrum from the light-on spectrum. The exact on/off durations are counted by DAQ clocks.

At the time of the measurements, the average Compton γ rate was 37.6 kHz above the energy threshold of 3 GeV, while the background rate was 3.6 kHz. The rate distributions obey Landau rather than Gauss statistics, with longer tails towards lower rates. With such a high threshold, only the Bremsstrahlung contributes to the background since the maximum energy of the scattered blackbody radiation is 0.73 GeV and the synchrotron radiation is absorbed in the preshower and the first tungsten plate of the calorimeter.

Additional details about the setup are available in refs. [20–23]

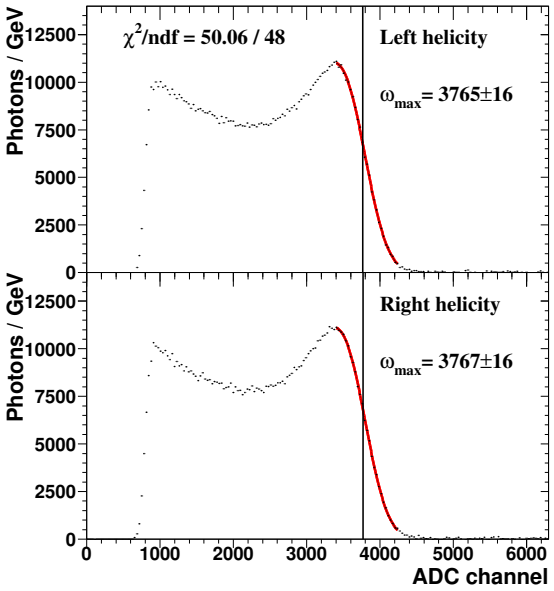

FIG. 3. Fitted Compton spectra from Fig. 2 *Inset*.

EXPERIMENTAL RESULTS

Method of Analysis. The raw spectra measured by the HERA transverse polarimeter are histograms with 8192 channels each (13 bit ADC). An example of a per-minute spectrum measured at 30/11/2006 during 23:41:33–23:42:33 is presented in Fig. 2 *Inset*. For this example, the laser-on (off) rate was 50.1(1.6) kHz and $1.1 \cdot 10^6$ high energy photons were collected for each helicity state (the *Inset a* displays only the left helicity spectrum). Algorithms for extracting the absolute maximum photon energy from the Compton and Bremsstrahlung spectra are described in ref. [4, 22]. Here we are interested in the Compton edge left-right helicity asymmetry so, we apply a simplified analyzing algorithm involving only the Compton spectra. After a reduction of the background subtracted Compton spectra to 256 bins both left and right spectra are fitted in a single MINUIT [24] run. The fitting function for each spectrum is a convolution of the theoretical Compton energy distribution $d\Sigma/d\omega$ with the detector response Gaussian function

$$F(E_a) = N_\lambda \int_0^{\omega_\lambda} \frac{d\Sigma}{d\omega} \frac{1}{\sqrt{\omega}} \exp\left(\frac{-(\omega - CE_a)^2}{2\sigma_0^2 \omega}\right) d\omega, \tag{11}$$

where σ_0 and E_a denote the calorimeter resolution and detected photon's energy in ADC units respectively. The normalizing factors $N_{+,-}$ and the maximum Compton energies $\omega_{+,-}$ are spectrum dependent. These four variables together with σ_0 and the calibration factor C are free parameters of the fit. The last two (detector) parameters can (slightly) change in the course of the lepton-fill or from fill to fill. The integral (11) for each MINUIT cycle is calculated numerically using Gaussian quadra-

ture. The Compton edge extraction fitting procedure is applied only to data within a narrow energy slice around the maximum energy to avoid contamination from systematic effects in the lower energy bins (see ref. [22]). Examples of fitted spectra (the same data as in Fig. 2 *Inset*) together with the fit outcome are displayed in Fig. 3. The quoted uncertainties are the statistical errors calculated by the fitting routine.

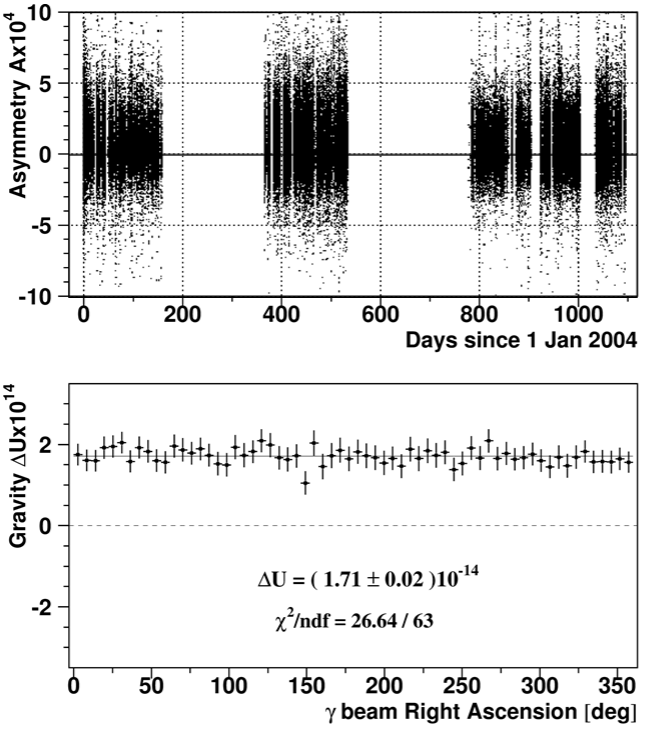

FIG. 4. *Upper plot:* Compton edge helicity dependent asymmetry measured by HERA transverse polarimeter. *Lower plot:* Angular dependence of the observed gravitational left–right potential difference.

Outcome of the measurements. Applying the described Compton edge extraction procedure to data collected during the 2004–2007 HERA running period, we succeeded in fitting 314,896 spectra complying with the standard criterium for p-values to exceed the threshold of 5%. Combining left and right helicity Compton edge values for each minute according to Eq. (8) we obtained 157,448 asymmetry points, plotted in Fig. 4 against their measurement time. Two extended gaps between the data points correspond to the accelerator shutdown periods. The average magnitude of the measured asymmetries weighted by inverse statistical errors is $(4.89 \pm 0.10) \cdot 10^{-5}$. From the observed asymmetry, we derive the gravitational left–right potentials difference $\Delta U_{\mathcal{P}}$ via Eq. (10). We also explore per-minute timestamps of the measurements to check how the asymmetry, or values of $\Delta U_{\mathcal{P}}$, are grouped relative to a fixed direction in space. For this purpose, we convert the timestamps T to Right Ascension (RA) angles in the celestial coordinate system by the formula $RA = 360^\circ \cdot T \pmod{T_S} - 9.87^\circ$, where T_S is the duration of the sidereal day and the angular offset is the polarimeter's setup longitude. While the rotation of the accelerator with the Earth sweeps the Compton beam along a circle on the celestial sphere, the declination angle of 33.35° stays constant. The resulting angular dependence reduced to 64 bins is shown in Fig. 4.

Systematic errors. The directional independence of the measured asymmetry is a validity check for the applied model. Indeed, observation of any preferred direction in space would violate the Lorentz symmetry (SR). Describing such a vectorial asymmetry that breaks the equivalence principle of GR together with the Lorentz invariance of SR would need a more complicated formalism than the applied scalar gravitational potentials' formulas. The observed asymmetry, however, is highly isotropic and this type of theoretical error can be safely ignored. We came to this conclusion by fitting the observed angular dependence with a constant for different binnings and comparing χ^2 to ndf (the values for 64 bins are displayed in Fig. 4).

Besides gravitation, other interactions also may alter the energy–momentum relation [25, 26]. For high energy processes, the main competitor to gravity would be a background electromagnetic field. As an example, let's estimate the influence of magnetic fields. According to Eq. (1.1) from ref. [25], the maximum impact on the energy–momentum relation for photons in a magnetic field B is given by

$$\frac{P}{\mathcal{E}} = 1 - \frac{11}{45}\frac{\alpha^2}{m^4}B^2, \tag{12}$$

where α is the fine structure constant. Hence, the refractivity created by a 4 T superconducting magnet is about $8{\cdot}10^{-21}$ and that of Earth's magnetic field is 10^{-25}. Magnetic refractivity's (transverse) spin asymmetry amounts to about one-half of the mentioned values or, more precisely, to the 6/11-th part. These tiny effects are still experimentally unreachable, and, compared to the magnitude of the gravitational potential (either the Local Supercluster's $\sim 10^{-5}$ or the Earth's $\sim 10^{-9}$) in Eq. (1), are completely negligible. The hypothetical influence of the helicity-dependent weak interaction is excluded by energy conservation: the weak bosons are too heavy to contribute to the Compton scattering at the HERA lepton energy scale, and, no virtual tree or loop heavy boson can shift the Compton edge. Thus, an impact on the Compton edge asymmetry from non-gravitational forces is largely ignorable.

Possible instrumental false asymmetries may arise from polarized effects correlated with the laser helicity flips. These are linked with the lepton's transverse or longitudinal spin and the laser light's linearly polarized fraction coupled to the gamma-calorimeter segmentation. The maximum possible theoretical asymmetries in po-

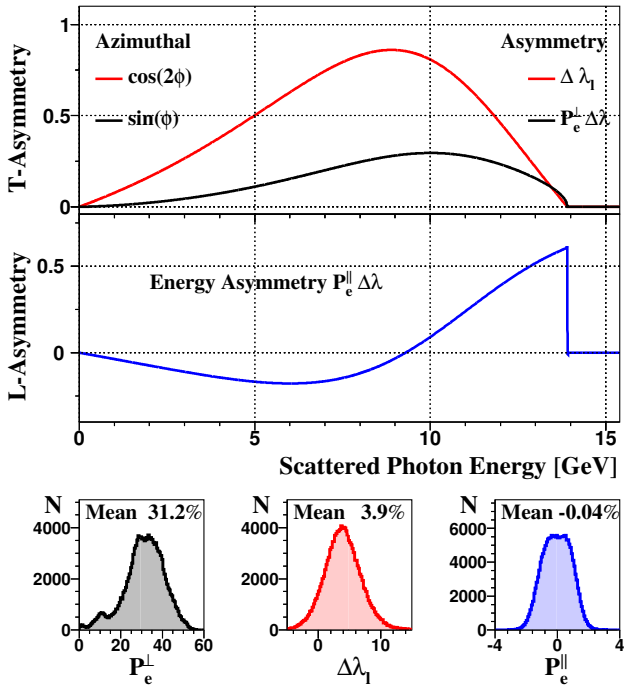

FIG. 5. *Upper rows:* Transverse-spatial (angular) and longitudinal-energy asymmetries in Compton scattering associated with the initial photon's polarization (linear λ_l and circular λ) flips. Analyzing powers (asymmetries for the cases $|P_e^{\parallel}\Delta\lambda| = 1, |\Delta\lambda_l| = 1, |P_e^{\perp}\Delta\lambda| = 1$) of the HERA transverse polarimeter setup. *Lower row:* Percent polarizations measured during 2004–2007.

larized Compton scattering at the HERA polarimeter are presented in Fig. 5. As follows from the plots, at the Compton edge energy, the influence of the longitudinal polarization of the electron beam ($P_e^{\parallel}$) is dominant while the contributions of the transverse polarization ($P_e^{\perp}$) and linear light (λ_l) drop to zero. Although none of the mentioned factors could physically alter the Compton gamma's maximum energy, the instrumental smearing can mimic a Compton edge shift, given a sufficiently large lepton beam polarization or linear light. In order to estimate the magnitude of these effects, we explored polarimeter detector simulation codes used in ref. [27] with $P_e^{\perp}$, $\Delta\lambda_l$ and $P_e^{\parallel}$ measurements (Fig. 5 *Lower row*). From simulated per-minute spectra ($1.2\cdot10^6$ photons per helicity state), the Compton edge asymmetry has been extracted applying the same algorithm as for the real data. For the simulated 100% $P_e^{\perp}$, $\Delta\lambda_l$ and $P_e^{\parallel}$ values the instrumental false asymmetries amount to $1.013 \cdot 10^{-5}$, $5.379 \cdot 10^{-6}$ and $4.625 \cdot 10^{-3}$ respectively. These numbers have been derived from 60,000 simulated spectra for each factor. Scaling the asymmetries by the observed average values for the 2004–2007 running period $< P_e^{\perp} >= 31.18\%$, $< \Delta\lambda_l >= 3.92\%$ and $< P_e^{\parallel} >= -0.038\%$, we get an estimate of the measured asymmetry instrumental error of $3.62 \cdot 10^{-6}$, where we chose a quadratic summation to neutralize the negative sign of the mean longitudinal polarization. Alternatively one can correct the observed asymmetry by the longitudinal polarization factor, assigning half of the correction magnitude as systematic error, and apply more conservative linear summation. This will enhance the observed asymmetry from $4.89 \cdot 10^{-5}$ to $5.07 \cdot 10^{-5}$ and will rise the instrumental error from $3.62 \cdot 10^{-6}$ to $4.25 \cdot 10^{-6}$. The most conservative method, however, is a linear summation of the errors' absolute values which brings the maximum instrumental error to $5.13 \cdot 10^{-6}$. Using this value together with the above quoted statistical uncertainty we get the measured asymmetry with an overall error of $(4.89 \pm 0.52) \cdot 10^{-5}$.

In order to evaluate the uncertainty of the $\Delta U_{\mathcal{P}}$ one needs to propagate the measurement errors from the asymmetry as well the kinematic and Lorentz factors through Eq. (10). Listing the errors of the x and γ factors' constituents yields $\sigma(\omega_0)/\omega_0 \approx 10^{-5}$, $\sigma(m)/m \approx 3 \cdot 10^{-7}$, $\Delta(\theta_0) \approx 2\ mrad \Rightarrow \Delta \sin^2(\theta_0/2) \approx 3 \cdot 10^{-6}$, $\sigma(\mathcal{E})/\mathcal{E} \approx 10^{-3}$, and we note that the dominant uncertainty comes from the HERA leptons' energy spread. The quoted systematic errors are collected in table II. Calculations with the displayed values give the measurement's final result: $\Delta U_{\mathcal{P}} = (1.71 \pm 0.036 \pm 0.187) \cdot 10^{-14}$, where the statistical and systematic errors are displayed separately.

TABLE II. Error bank of the measurements of the Compton edge asymmetry and difference between the gravitational potentials.

Source	Magnitude	Error ΔA
Magnetic field	50 μT	$5.5 \cdot 10^{-26}$
Transverse polarization	31.2%	$3.2 \cdot 10^{-6}$
Laser linear polarization	3.9%	$2.1 \cdot 10^{-7}$
Longitudinal polarization	-0.04%	$1.8 \cdot 10^{-6}$
	Magnitude (rel.)	Error $\Delta U_{\mathcal{P}}$
Statistical fluctuations	$2.1 \cdot 10^{-2}$	$3.6 \cdot 10^{-16}$
Laser frequency shift	10^{-5}	$1.7 \cdot 10^{-19}$
Electron mass error	$3 \cdot 10^{-7}$	$1.0 \cdot 10^{-20}$
Interaction angle drift	$3 \cdot 10^{-6}$	$5.2 \cdot 10^{-20}$
HERA-e energy spread	10^{-3}	$3.8 \cdot 10^{-17}$
Asymmetry measurement	0.11	$1.9 \cdot 10^{-15}$

This measurement, as a by-product of the HERA polarimetry, may also suffer from hidden systematic factors such as the major suspects – the detector's helicity dependent gain or the lepton beam non-gaussian deviations in 6D phase-space convoluted with a possible laser spatial jitter at IP which is correlated with the light polarization [28]. For the gain effects we have estimates from the bremsstrahlung edge fits [22] to be of the opposite sign (on average) to the observed asymmetry. De-

tailed corrections which on average will enhance the observed asymmetry, are, however, complicated since the bremsstrahlung and Compton beams have an unknown mutual offset on the face of the spatially inhomogeneous calorimeter. For the lepton and the polarized laser beam spatial convolution the estimations are more complex if the optical jitter helicity dependent direction, averaged over the four years period, would differ considerably from a plausible zero value. The mentioned and other possible hidden effects, which could have been measured or controlled during the machine operation, are out of experimental reach since the HERA is stopped in 2007.

CHIRAL GRAVITY IMPLICATIONS

The main message of the observed parity violation is that gravitational equivalence is broken and systems or processes involving spin are gravity dependent. Although experimental detection is made at high energy, 13.9 GeV, gravity's universality, infinite range, and all-attractive nature suggest an energy independence of the observed helicity preference of gravitation.

This would mean that the hydrogen atom's well known electron–proton spin radiation (21 cm line) will be affected by the gravitational potential at the location of the atom. So far, the observed deviations from the 21 cm line have been attributed to Doppler shifted velocities to infer the presence of dark matter [29]. Meanwhile, the detected chiral gravity could possibly explain the galaxies' anomalous rotational curves by differences in the gravitational potentials at the Earth (where the 21 cm line is calibrated) and the periphery of the galaxy. Detailed calculations are outside the scope of this paper. Besides, the uncertainties in the gravitational potentials, whether in galaxies or even at the Earth, seem too large for an accurate answer.

At the nuclear level, the helium nucleus in a gravitational field will emit photons with energy $2\Delta U_{\mathcal{P}} \cdot M_D$, where M_D is the deuteron mass. The radiation will be induced by different gravitational couplings for two opposite spin deuterons composing the helium. According to the potentials quoted in table I, at the Earth's surface the radiation frequency is around 16 GHz, which is only an order of magnitude away from the peak frequency of the Cosmic Microwave Background (CMB, currently assumed as a Big Bang remnant). This fact, together with the estimated helium abundances of 25% in the universe [30], hints that a considerable part of the CMB could originate from the wide variety of gravitational potentials in which the helium nuclei are located, distributed according to blackbody radiation statistics. An observation of the corresponding background blackbody radiation from helium electrons' opposite spins (energy $2\Delta U_{\mathcal{P}} \cdot m$), with peak frequency reduced by a factor m/M_D, could confirm this hypothesis. An excess of radiation at the CMB 2.73 K spectrum low frequencies [3], observed in 2011 by the ARCADE collaboration [31], could already be a signature of the helium electrons' spin 0.74 mK spectrum's high frequency tail.

At scales larger than the atomic, one could possibly find an influence of chiral gravity on asymmetric chemical and helical molecules of life. These, however, are composite complex systems and the interaction is more difficult to justify and quantify.

CONCLUSIONS

The indication of a spin dependence of gravitation, found earlier in a limited amount of data, has been confirmed by the analysis of four years of data from the HERA transverse polarimeter. A left–right helicity asymmetry at the kinematic edge of the Compton scattered γ-quanta is established with a 9σ confidence level. According to the described formalism, this asymmetry is induced by the breaking of gravitational equivalence: the interaction's intensity depends on the helicity. The contributions of the other three fundamental interactions to this asymmetry has been proven to be negligibly small.

Further experimental investigations of gravity's spin preference could be done at high-γ accelerators or with atomic and nuclear quantum experiments if sufficient sensitivity could be achieved. The latter possibility assumes an energy independence of the observed effect, which would suggest revisiting the hydrogen 21 cm line spectroscopy data so as to disentangle the contributions of the gravitational fields from that of the Doppler velocities. Within radio astronomy, the feasibility of detection of the possible 0.74 mK background radiation could be evaluated as well.

ACKNOWLEDGEMENT

We are thankful to the machine staff and all H1, HERMES, ZEUS collaborators who have contributed to the setup and data taking of the HERA transverse polarimeter.

[1] A. Einstein, Annalen Phys. **49**, 769 (1916).
[2] C. M. Will, Living Rev. Rel. **17**, 4 (2014) doi:10.12942/lrr-2014-4 [arXiv:1403.7377 [gr-qc]].
[3] C. Patrignani *et al.* [Particle Data Group], Chin. Phys. C **40**, no. 10, 100001 (2016). doi:10.1088/1674-1137/40/10/100001
[4] V. Gharibyan, DESY-M Preprint Hamburg: DESY-16-014 (2016) [PUBDB-2016-01182]
[5] B. R. Heckel, E. G. Adelberger, C. E. Cramer, T. S. Cook, S. Schlamminger and U. Schmidt, Phys. Rev. D **78** (2008) 092006 [arXiv:0808.2673 [hep-ex]].

[6] V. A. Kostelecky, Phys. Rev. D **69** (2004) 105009
[7] F. W. Hehl, P. Von Der Heyde, G. D. Kerlick and J. M. Nester, Rev. Mod. Phys. **48** (1976) 393.
[8] J. E. Moody and F. Wilczek, Phys. Rev. D **30** 130 (1984).
[9] W. T. Ni, Rept. Prog. Phys. **73** (2010) 056901 [arXiv:0912.5057 [gr-qc]].
[10] J. C. Evans, P. M. Alsing, S. Giorgetti and K. K. Nandi, Am. J. Phys. **69**, 1103 (2001) [gr-qc/0107063].
[11] R. V. Pound and G. A. Rebka, Phys. Rev. Lett. **3**, 439 (1959). doi:10.1103/PhysRevLett.3.439
[12] W. H. McMaster, Rev. Mod. Phys. **33** (1961) 8.
[13] G. L. Kotkin, V. G. Serbo and V. I. Telnov, Phys. Rev. ST Accel. Beams **6**, 011001 (2003) [hep-ph/0205139].
[14] F. W. Lipps, H. A. Tolhoek, Physica **20** (1954) 85, 385.
[15] P. L. Anthony *et al.* [SLAC E158 Collaboration], Phys. Rev. Lett. **92**, 181602 (2004) doi:10.1103/PhysRevLett.92.181602 [hep-ex/0312035].
[16] P. L. Anthony *et al.* [SLAC E158 Collaboration], Phys. Rev. Lett. **95** (2005) 081601.
[17] F. E. Maas [A4 Collaboration], Eur. Phys. J. A **24S2**, 47 (2005).
[18] F. E. Maas [A4 Collaboration], AIP Conf. Proc. **1056**, 98 (2008).
[19] S. Baudrand *et al.*, JINST **5**, P06005 (2010) doi:10.1088/1748-0221/5/06/P06005 [arXiv:1005.2741 [physics.ins-det]].
[20] D. P. Barber *et al.*, Nucl. Instrum. Meth. A **329**, 79 (1993).
[21] M. Lomperski, DESY-93-045
[22] V. Gharibyan, Phys. Lett. B **611** (2005) 231.
[23] B. Sobloher, R. Fabbri, T. Behnke, J. Olsson, D. Pitzl, S. Schmitt and J. Tomaszewska, arXiv:1201.2894 [physics.ins-det].
[24]
[24] F. James and M. Roos, Comput. Phys. Commun. **10**, 343 (1975). doi:10.1016/0010-4655(75)90039-9
[25] J. I. Latorre, P. Pascual and R. Tarrach, Nucl. Phys. B **437**, 60 (1995) [hep-th/9408016].
[26] W. Dittrich and H. Gies, Phys. Rev. D **58**, 025004 (1998) [hep-ph/9804375].
[27] V. Gharibyan and S. Schmitt, HERMES Internal Report 06-104, (2006), `http://www-hermes.desy.de/notes/pub/06-LIB/vahag.06-104.tpol-syserr.pdf`.
[28] R. Brinkmann, DESY, private communication, 2018.
[29] M. Persic, P. Salucci and F. Stel, Mon. Not. Roy. Astron. Soc. **281**, 27 (1996) doi:10.1093/mnras/281.1.27, 10.1093/mnras/278.1.27 [astro-ph/9506004].
[30] E. Aver, K. A. Olive and E. D. Skillman, JCAP **1005**, 003 (2010) doi:10.1088/1475-7516/2010/05/003 [arXiv:1001.5218 [astro-ph.CO]].
[31] D. J. Fixsen *et al.*, Astrophys. J. **734**, 5 (2011) doi:10.1088/0004-637X/734/1/5 [arXiv:0901.0555 [astro-ph.CO]].